

A Model Allowing for the Influence of Geometry and Stress in the Assessment of Fatigue Data

**Constanze Przybilla^{1,2,*}, Roland Koller²,
Alfonso Fernández-Canteli¹, Enrique Castillo³**

¹ Department of Construction and Manufacturing Engineering, University of Oviedo, 33203 Gijón, Spain

² Laboratory for Mechanical Systems Engineering, EMPA, 8600 Dübendorf, Switzerland

³ Department of Applied Mathematics and Computational Sciences, University of Cantabria, 39005 Santander, Spain

* Corresponding author: przybillaconstanze@uniovi.es

Abstract Usually, the Wöhler field of a material is obtained from fatigue lifetime data resulting from testing specimens of reduced size in the laboratory. This basic information finds subsequent application in lifetime prediction of larger structural and mechanical components. Thus, an important question arises: how can the S-N field be transformed into an ideal one referred to a characteristic size (length, area or volume) subjected to a constant stress distribution in order to achieve a safe structural integrity design?

In this work, the influence of specimen geometry and variable stress state on the fatigue lifetime distribution for constant amplitude fatigue tests is investigated. An experimental program has been carried out with unnotched specimens of nominally the same material but differing in length, diameter, and shape.

The experimental data is fitted to a newly developed fatigue model, capable of describing the S-N-field in a probabilistic manner accounting for both the specimen geometry and the variable stress state of the specimens. As the estimated Wöhler field is referred to an elemental surface, loaded by a constant stress level $\Delta\sigma$, the extrapolation of the fatigue resistance to different specimen geometries is possible. Additionally, problems encountered due to scatter of the material properties are discussed.

Keywords SN curves, Size effect, Probabilistic modelling, Transferability, Specimen geometry

1. Introduction

It has been observed that fatigue lifetime depends on the size of the structural element, whereby larger specimens present lower fatigue lifetime than smaller ones when loaded by the same stress range. This so-called size effect stems from the higher probability of larger specimens to contain a critical crack, capable of initiating the fatigue process, compared to smaller specimens. Investigations on the size effect in fatigue have been done, amongst others, by Weibull [1] on ball bearing steel, by Picciotto [2] on yarn, by Köhler [3] on wires and flat specimens, by Fernández-Canteli et al. [4] on prestressing wires and by Shirani et al. [5] on wind turbine castings. Understanding the size effect is crucial to extrapolate fatigue data from small specimens tested in the laboratory to real structures. Additionally, specimen geometries used in fatigue experiments sometimes present a cross-section with varying diameter along their lengths (see Fig. 2). The experimental results ($\Delta\sigma$ versus lifetime N) obtained from testing these specimens are usually evaluated considering the maximum nominal stress range $\Delta\sigma_0$ acting in the smallest cross section and the stress ratio $R = \sigma_{min}/\sigma_{max}$. While the stress ratio R is the same for all cross sections, $\Delta\sigma$ varies along the specimen length. Thus, even if a specimen is likely to fail in the section with the highest $\Delta\sigma$, the remaining sections with lower $\Delta\sigma$ influence the overall failure probability. That is why for a specimen as depicted in Fig. 2 it is statistically not correct to refer the results only to the surface or volume with the smallest radius (central section). Though there are models to account for the pure length effect, e.g. [6], the variable stress in the specimen is in general not accounted for.

The present investigation proposes a new model to evaluate fatigue test data considering both size effect and variable stress state of the test specimens. This allows, on one hand, a comparison of fatigue data obtained for different specimen sizes and, on the other hand, to establish a new method to extrapolate fatigue life results from laboratory tests to different specimen sizes and real structures. The applicability of the model is checked by evaluating three experimental fatigue data

sets corresponding to three specific specimen geometries of the same material: the aluminium alloy AlMgSi1-6082.

2. Model proposal

In this section a new method to evaluate fatigue data is presented which extends the applicability of the probabilistic fatigue model presented by Castillo and Fernández-Canteli [6] for a more general description of the fatigue behaviour considering specimen geometry, i.e. size effect and variable stress state.

2.1. Probabilistic model

The Weibull regression model described in [6] is based on physical and statistical assumptions. The compatibility condition between the probability distributions present in the Wöhler field, i.e. the probability distribution $P_f(\Delta\sigma|N)$ of $\Delta\sigma$ for constant N and the probability distribution $P_f(N|\Delta\sigma)$ of N for constant values of $\Delta\sigma$, plays an important role, manifesting that the values of the failure probability for every combination of $\Delta\sigma$ and N must be equal for $P_f(\Delta\sigma|N)$ and $P_f(N|\Delta\sigma)$. The model describes the Wöhler field in a probabilistic way by means of percentile curves, i.e. curves representing a constant failure probability, and computes the failure probability $P_f(N, \Delta\sigma)$ for a combination of stress range $\Delta\sigma$ and number of cycles N by

$$P_f(N, \Delta\sigma) = 1 - \exp \left[- \left(\frac{((\ln N - B)(\ln \Delta\sigma - C) - \lambda)}{\delta} \right)^\beta \right], \quad (1)$$

which corresponds to a three-parameter Weibull distribution of the variable $V = (\ln N - B)(\ln \Delta\sigma - C)$ with location parameter λ , shape parameter β , and scale parameter δ [7]. V represents a normalizing variable and could be interpreted as a damage parameter. B and C are the threshold parameters for lifetime and stress range, respectively. Fig. 1 gives an example of the model depicting the SN field on the left and the normalized variable on the right. A detailed description of the model can be found in [6].

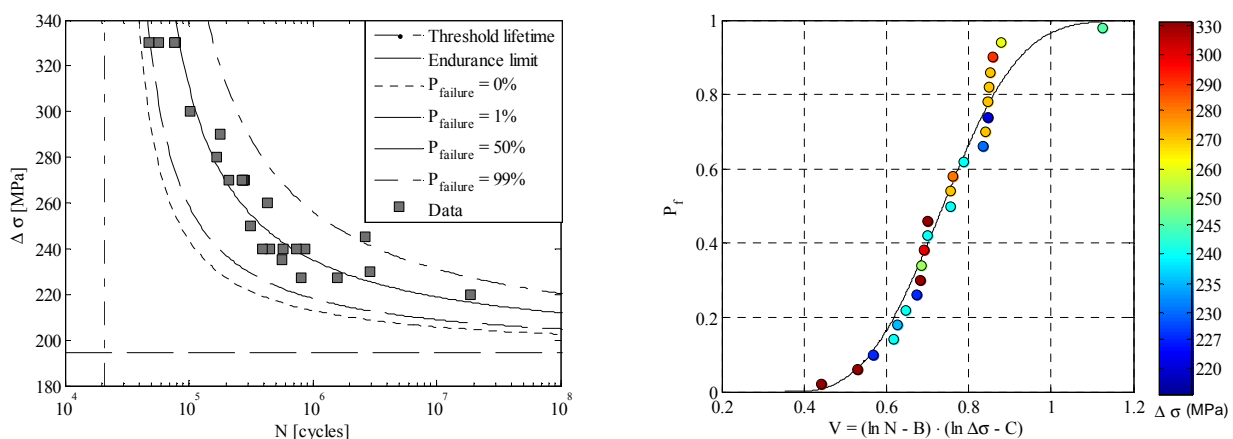


Figure 1. SN field and normalized variable V

2.2. Consideration of size effect and variable stress state

In principle the fatigue life depends not only on the material, the stress range, and the stress ratio, but also on the specimen length, as found for example in [4]. This means that the longer a specimen the higher the failure probability if the same stress range $\Delta\sigma$ is applied. This phenomenon, called statistical size effect, is due to the fact that a larger specimen is more likely to contain a large critical crack than a smaller specimen, cracks being considered to originate fatigue failure. Furthermore, specimen geometries used in fatigue experiments frequently present a cross-section with varying diameter along their lengths (see Fig. 2). The experimental results ($\Delta\sigma$ versus lifetime N) stemming from testing these specimens are usually evaluated considering only the maximum stress range $\Delta\sigma_0$, acting on the smallest cross section, and the stress ratio $R = \sigma_{min}/\sigma_{max}$. While the stress ratio R is the same for all cross sections, $\Delta\sigma$ is varying along the specimen length. To extrapolate from those test results to structural elements or specimens of different size it is advantageous to obtain a “normalized” Wöhler field. To accomplish this task a new method is developed, based on the following assumptions:

- Fatigue failure initiates from surface flaws. Therefore the size effect is related to the stressed surface area, i.e. the larger the stressed surface the higher is the failure probability for the same combination of $\Delta\sigma$ and N .
- Validity of statistical independence and weakest-link principal implying that the survival probability $P_{s,S}$ of a surface $S = n \cdot S_i$ composed of n surface elements of size S_i is given by the product of the individual survival probabilities P_{s,S_i} of the subelements each loaded by a stress range $\Delta\sigma_i$, i.e.

$$P_{s,S}(N, \Delta\sigma) = \prod_{i=1}^n P_{s,S_i}(N, \Delta\sigma_i). \quad (2)$$

Accordingly, if all surface elements have the same size S_i and are loaded by the same stress range $\Delta\sigma_i$ one gets

$$P_{s,S}(N, \Delta\sigma) = \left(P_{s,S_i}(N, \Delta\sigma_i) \right)^{S/S_i}. \quad (3)$$

- For the moment, only the uni-axial load case is considered, so that Eq. (1) describes the failure probability $P_{f,\Delta S}$ for a uni-axially tensioned surface element ΔS .

With those assumptions and $P_{s,\Delta S} = 1 - P_{f,\Delta S}$ we can combine Eqs. (1) and (3) to obtain the survival probability for a uni-axially tensioned surface element of size $S_i = n_i \cdot \Delta S$ as

$$P_{s,S_i}(N, \Delta\sigma) = \left(1 - P_{f,\Delta S}(N, \Delta\sigma) \right)^{S_i/\Delta S} = \exp \left[- \frac{S_i}{\Delta S} \left(\frac{(\ln N - B)(\ln \Delta\sigma - C) - \lambda}{\delta} \right)^\beta \right] \quad (4)$$

Thus, for an arbitrary structure under fatigue load with tensioned surface $S = n \cdot S_i$ composed of n surface elements of size S_i , each loaded by a different stress level $\Delta\sigma_i$, combining Eqs. (2) and (4) one gets

$$\begin{aligned}
 P_f(N, \Delta\sigma_0) &= 1 - \prod_{i=1}^n \exp \left[-\frac{S_i}{\Delta S} \left(\frac{(\ln N - B)(\ln \Delta\sigma_i - C) - \lambda}{\delta} \right)^\beta \right] \\
 &= 1 - \exp \left[-\sum_{i=1}^n \frac{S_i}{\Delta S} \left(\frac{(\ln N - B)(\ln \Delta\sigma_i - C) - \lambda}{\delta} \right)^\beta \right]
 \end{aligned} \quad (5)$$

For a specimen with circular cross section and variable diameter $d(x)$ over its length, being d_0 the minimal diameter in the section loaded by the maximum stress level $\Delta\sigma_0$, the summation can be extended to an integral. With $S_i = \pi d(x) dx$, we get

$$P_f(N, \Delta\sigma_0) = 1 - \exp \left[-\frac{2\Pi}{\Delta S} \int_0^{UB} \left(\frac{(\ln N - B) \left(\ln \left(\Delta\sigma_0 \frac{d_0^2}{d(x)^2} \right) - C \right) - \lambda}{\delta} \right)^\beta d(x) dx \right] \quad (6)$$

Due to symmetry, the integration is carried out over half the specimen length starting in the centre of the specimen, being the upper integration bound UB the x-coordinate, where $(\ln N - B)(\ln(\Delta\sigma(x)) - C) = \lambda$.

2.3. Effective surface area

For a specimen under variable stress state an effective specimen surface S_{eff} can be defined having the same failure probability as the whole specimen but subjected to a constant stress range $\Delta\sigma$. The normalizing variable for the nominal maximum stress $\Delta\sigma_0$ acting in the central section of the specimen with diameter d_0 is represented by $V_0 = (\ln N - B)(\ln \Delta\sigma_0 - C)$. For different specimen sections with diameter $d(x)$ we have $V(x) = (\ln N - B)(\ln(\Delta\sigma_0 \cdot d_0^2/d(x)^2) - C)$. An analytical expression for S_{eff} is obtained equating Eqs. (5) (with $S_i = S_{eff}$) and (6):

$$S_{eff} = \frac{2 \Pi \int_0^{UB} (V(x) - \lambda)^\beta d(x) dx}{(V_0 - \lambda)^\beta} \quad (7)$$

As can be observed from Eq. (7) S_{eff} is independent of δ but depends on the parameters B , C , λ and β of the Weibull model and also on the number of cycles N and the stress range $\Delta\sigma$. For given values of N and $\Delta\sigma_0$ and known material parameters B , C , λ and β the effective surface and the failure probability can be computed. However, for a specific specimen S_{eff} cannot be calculated directly from the failure data, since the Weibull parameters are still unknown. Thus, an iterative process, as explained in [8], is used for the parameter estimation. Firstly, the n test data are fitted to the model given by Eq. (1), then the normalized values V_0 are assigned their accumulated failure probabilities by $P_f = (i - 0.3)/(n + 0.4)$. To refer the data to the surface element ΔS , those failure probabilities

are shifted by using $P_{f,i,\Delta S} = 1 - \left(1 - P_{f,i,S_{eff}} \right)^{\Delta S/S_{eff,i}}$. The $V_{0,i}$ and their corresponding $P_{f,i,\Delta S}$ are fitted to a three-parameter Weibull distribution. The obtained values for λ and β are used to update the effective surface given by Eq. (7) in each iteration loop. Those steps are repeated until the Weibull parameters converge.

3. Material and experimental programme

To investigate the influence of the size effect and the variable stress state on the fatigue behaviour, specimens with different geometries have been tested until complete fracture at EMPA-Dübendorf (Swiss Federal Material Testing and Research Laboratories). All specimens whose dimensions are given in table 1 and refer to Fig. 2 have been machined by the same manufacturer from rods of the aluminium alloy AlMgSi1 6082-T6 with chemical composition given in table 2. The d3 and d8 specimens were machined from rods of diameter 25 mm and the d22 specimens from rods with diameter 45 mm. The corresponding yield and ultimate strengths are given in table 2 as the mean of three values obtained from static strength tests using normalized specimens.

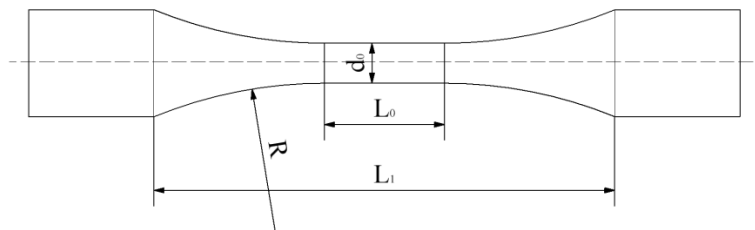


Figure 2. Specimen geometry

Table 1. Tested specimen geometries

Name	d_0 [mm]	L_0 [mm]	L_1 [mm]	R [mm]
d3	3	0	22.4	24
d8	8	24	88.6	90
d22	22	240	385.0	245

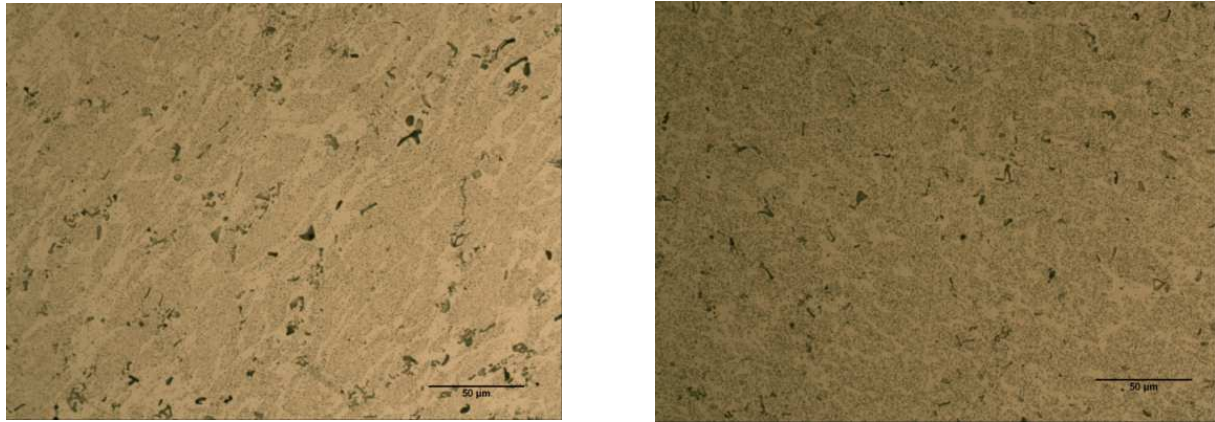
Table 2. Chemical composition and strength of AlMgSi1 6082-T6

d [mm]	Si [%]	Fe [%]	Cu [%]	Mn [%]	Mg [%]	Cr [%]	Zn [%]	Ti [%]	Pb [%]	R_m [MPa]	$R_{p0.2}$ [MPa]
25	1.002	0.499	0.091	0.749	0.831	0.032	0.186	0.063	0.026	410	402
45	0.850	0.280	0.060	0.430	0.710	0.050	0.050	0.030	N/A	369	350

Since the static strength of the specimens differs for the different rods, additionally micrographies were taken (one from each rod) as shown in Fig. 3. It can be observed that the microstructure happens to be quite similar for both samples, thus, justifying a direct comparison of the fatigue test data.

The constant amplitude fatigue tests were carried out in pure tension with a stress ratio $R=0.1$. For the tests of the d3 and d8 specimens resonance frequency machines (Rumul) equipped with 5 kN and 100 kN load cells, respectively, were used, whereas the d22 specimens were tested by a servo-hydraulic machine (Schenck) with 630 kN load cell. The forces were calculated taking into account the measured diameters in the central section of each specimen and the stress ranges $\Delta\sigma$, to be applied in this section. For all specimens the difference between measured and nominal diameter was less than 0.03 mm. The predominant role of the surface flaws has been corroborated by ocular

and microscopic inspection of the failure sites revealing that the practical totality of the fatigue failures started from the specimen surface. In the exceptional case that a failure could be identified to have its origin in a volume defect, it was not considered in the present analysis.



a) Rod $d=25$ mm (used for d3 and d8 specimens)

b) Rod $d=45$ mm (used for d22 specimens)

Figure 3. Microstructure of AlMgSi

4. Results and model application

The experimental data sets for each specimen geometry were individually fitted to the model given by Eq. (6) of section 2.2. to obtain the parameters referred to $\Delta S=9$ mm² as shown in table 3. The choice of ΔS is free, so that larger values of ΔS will only result in smaller values of δ , remaining the other parameters unchanged.

Table 3. Parameter estimates for each data set

d_{min} [mm]	ΔS [mm ²]	B	$\exp(B)$ [cycles]	C	$\exp(C)$ [MPa]	λ	β	δ
3	9	11.57	105873	5.40	221	0.01	2.42	0.16
8	9	9.95	20952	5.27	194	0.21	4.31	1.65
22	9	10.63	41357	5.27	194	0.00	3.41	4.09

The fatigue test data and their corresponding Wöhler fields are represented in Fig. 4 for the specimen geometries d3, d8, and d22. The percentiles are computed replacing into Eq. (6) the parameter estimates referred to the area ΔS given in table 3 and the specimen geometries of table 1. In a second step, the SN fields for the d3 and d22 specimens are predicted based on the parameter estimates, found by fitting the data of another specimen geometry, by substituting the corresponding radii and lengths in Eq. (2). Figs. 5a and b show the Wöhler fields for the d3 and d22 specimens using the parameter estimates obtained by fitting the d8 data. The extrapolations from the d3 to the d22 specimen and from the d22 to the d3 specimen are given in Figs. 5c and d, respectively.

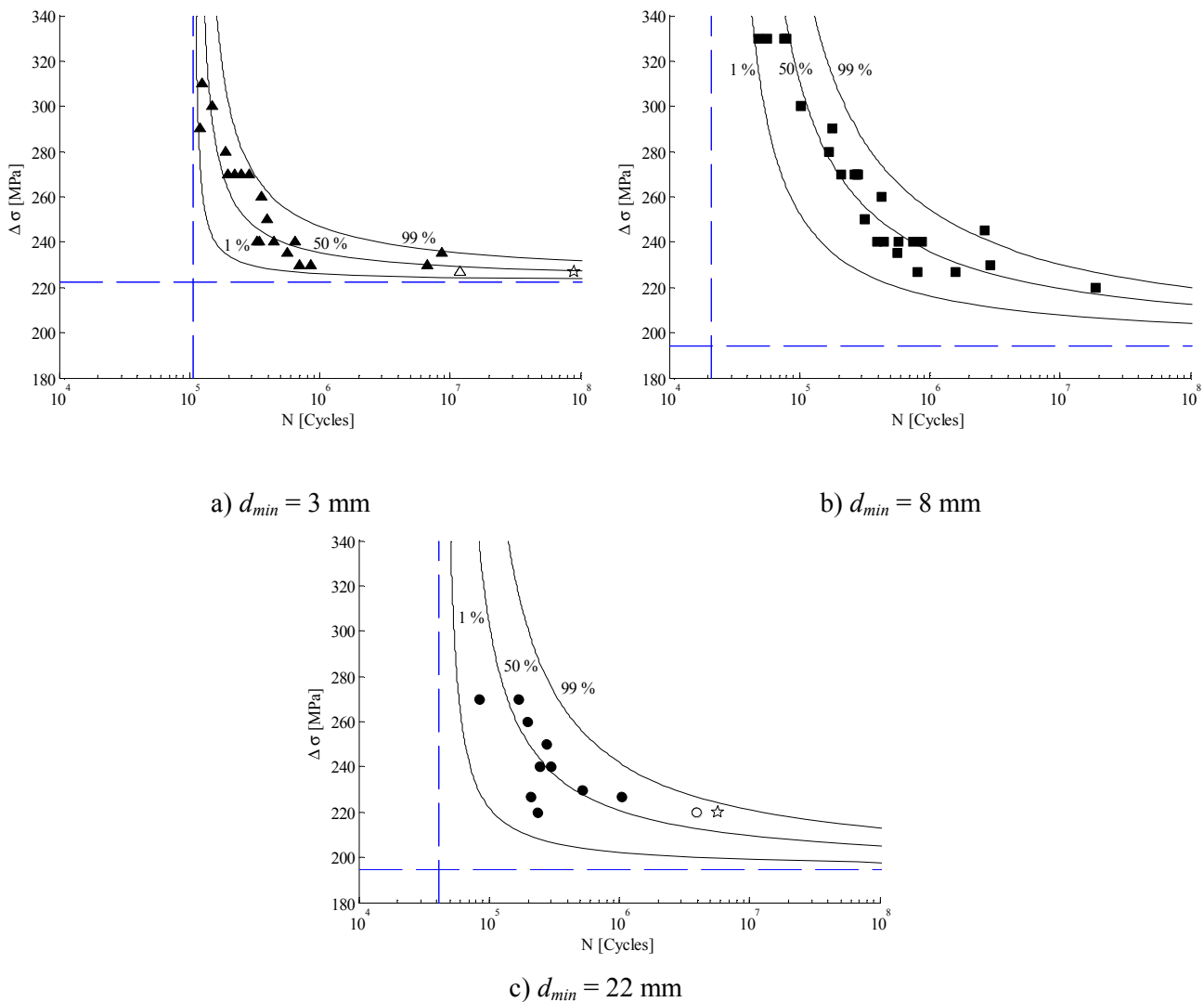


Figure 4. AlMgSi1 fatigue data and percentile curves for 1, 50 and 99 % failure probability

5. Discussion

As can be observed in Fig.4, the percentile curves for all three specimen geometries provided by the model describe the fatigue data well, both in terms of median curve and data scatter. As the estimated parameters for each data set are referred to the same surface area ΔS , they should coincide for all three data sets. Nevertheless, as can be seen in table 3, this is only the case for the threshold parameter C for the d8 and d22 specimens. According to the model, a comparison of the Weibull parameters λ , β and δ requires the parameters B and C to be coincident to compute the normalized variable V .

The extrapolation from the d8 estimates to the d3 Wöhler field overestimates both the median curve of fatigue life for constant stress levels and the data scatter. A possible reason could be that for such small specimens statistical independence, as is an assumption of the model, is not fulfilled in this case. As reference for other practical cases, in [6] it was also observed that the fatigue behaviour of the shortest prestressing wires could not be described based on the estimates for the longer wires. Therefore, the statistical dependence [9] based on considerations related to the defects from which fatigue initiation arises together with experimental work should be further investigated in order to

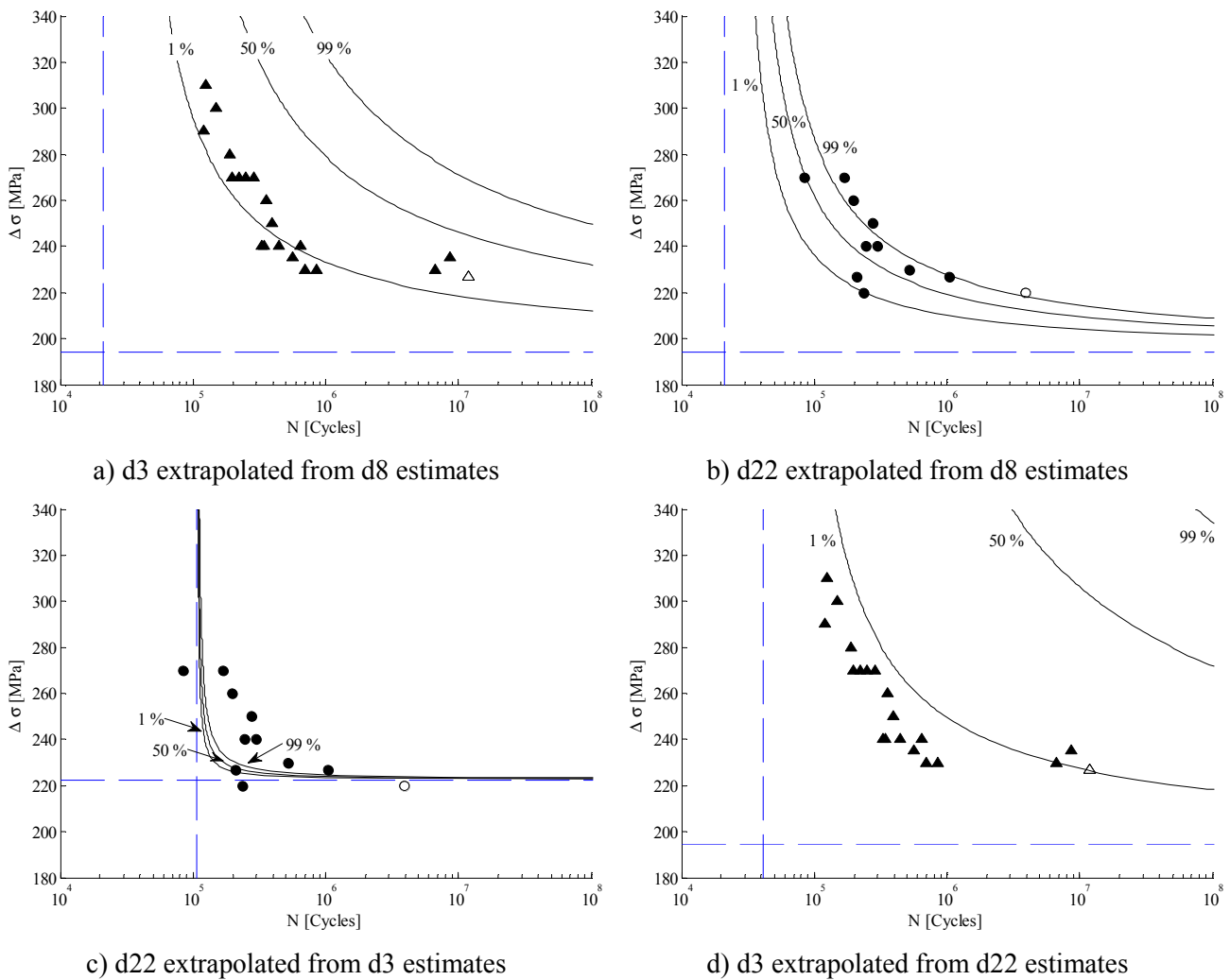


Figure 5. Extrapolation to different specimen geometries (1, 5 and 99 % percentile curves)

improve the model. Different surface quality can also be excluded, as all specimens were machined in the same workshop, therefore supposedly having undergone the same surface treatment. In particular, both the d3 and d8 specimens were fabricated from 25 mm diameter rods. Although, this implies that the surface of the d3 specimens is closer to the centre of the rods than the surface of the d8 specimens and possibly having experienced both different cooling rates, the difference is negligible bearing in mind the original rod diameter.

One could also question the existence of a size effect. Though this assumption might be true for the d3 and d8 specimens, it is obvious from Fig. 6 that the d22 specimens have lower lifetimes than the d3 and d8 specimens for the same stress ranges. Nevertheless, in the region of low stress ranges, the d3 specimens tend to present higher fatigue lifetimes than the d8 specimens.

On the other hand, the prediction for the d22 specimens based on the d8 estimates (Fig. 5b) is quite good lying almost all failure data for the d22 specimens between the 1 and 99 % - percentiles. However, a tendency to underestimate the fatigue strength is noticeable since by the extrapolation the data with highest lifetime are assigned to failure probabilities higher than 99 %.

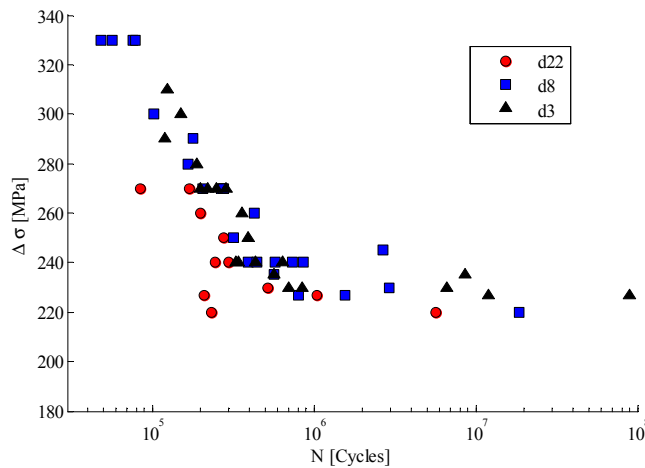


Figure 6. AlMgSi1 fatigue data for the tested specimen geometries

The extrapolation to the d22 specimen geometry based on the d3 estimates (Fig. 5c) leads to an underestimation of the data scatter and of the median curve. In this context, it has to be noted that the threshold parameters for the d3 data set were estimated in higher values than those for the d8 and d22 data sets. In fact, the threshold stress $\exp(C)$ for the d3 specimens results in 221 MPa which represents a higher value than the lowest stress range in the fatigue results for the d8 and d22 specimens equal to 220 MPa. Therefore, failure data lying below the threshold stress of the estimated model cannot be represented by the model. In contrast, the prediction of the SN field for the d3 geometry based on the d22 estimates (Fig. 5d) results in a noticeable overestimation of mean curve and data scatter.

6. Conclusions

A new model for the evaluation of fatigue test results under simultaneous consideration of size effect and variable stress state along the specimens is presented. The model, describing the SN field by means of percentiles, has been applied to three sets of fatigue data for AlMgSi1, each set obtained on specimens with different size. The estimated SN fields fit the experimental data well. As the parameters of the fatigue model are referred to a uni-axially and uniformly tensioned surface element, extrapolation to different specimen geometries can be performed. However, extrapolation to different specimen geometries is only satisfactory from the d8 to the d22 specimens. For the other presented cases, an extrapolation of the model from larger to smaller specimens overestimates the lifetimes of the smaller specimens and vice versa, an extrapolation from smaller to larger specimens tends to underestimate the fatigue behaviour. Thus, further research will be undertaken to get a deeper understanding of the size effect, and the role played by the defect distribution and the statistical independence assumption in order to improve the model.

Acknowledgements

The authors are indebted to the MICINN (Ministry of Science and Innovation) (Project BIA2010-19920) for financial support of this work. Furthermore, we thank Ing. Ana Teresa Vielma Mendoza for her help in the preparation of the micrographies.

References

- [1] W. Weibull. A statistical representation of fatigue failures in solids. Technical report, Royal Institute of Technology of Sweden, 1949.
- [2] R. Picciotto. Tensile fatigue characteristics of sized polyester/viscose yarn and their effect on weaving performance. PhD thesis, North Carolina State University, 1970.
- [3] J. Köhler. *Statistischer Größeneinfluss im Dauerschwingverhalten ungekerbter und gekerbter metallischer Bauteile*. PhD thesis, TU München, 1975.
- [4] A. Fernández-Canteli, V. Esslinger, and B. Thürlimann. Ermüdungsfestigkeit von Bewehrungs- und Spannstählen. Technical report, Institut für Baustatik und Konstruktion ETH Zürich, 1984.
- [5] M. Shirani and G. Härkegård. Fatigue life distribution and size effect in ductile cast iron for wind turbine components. *Engineering Failure Analysis*, 18(1):12 – 24, 2011.
- [6] E. Castillo and A. Fernández-Canteli. *A Unified Statistical Methodology for Modeling Fatigue Damage*. Springer, 2009.
- [7] W. Weibull. A statistical theory of the strength of materials. *Proc Roy Swed Inst Eng Res*, (151):1 – 45, 1939.
- [8] C. Przybilla, A. Fernández-Canteli, and E. Castillo. Deriving the primary cumulative distribution function of fracture stress for brittle materials from 3- and 4-point bending tests. *Journal of the European Ceramic Society*, 31:451–60, 2011.
- [9] E. Castillo, A. Fernández-Canteli, J. Ruiz-Tolosa, and J. Sarabia. Statistical models for analysis of fatigue life of long elements. *Journal of Engineering Mechanics*, 116(5):1036–1049, 1990.